Performance and emissions of renewable blends with OME3-5 and HVO in heavy duty and light duty compression ignition engines

N.B. When citing this work, cite the original published paper.

(article starts on next page)
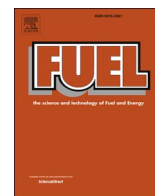
Full Length Article

Performance and emissions of renewable blends with OME$_{3-5}$ and HVO in heavy duty and light duty compression ignition engines

Josefine Preuß [*], Karin Munch, Ingemar Denbratt

Chalmers University of Technology, Gothenburg, Sweden

ARTICLE INFO

ABSTRACT

Interest in poly(oxymethylene)dimethyl ether (OME$_{3-5}$) as an alternative to fossil fuels in compression ignition engines has increased owing to its potential for soot reduction. The high oxygen content of the polymer and lack of carbon–carbon bonds and aromatic structures can help to reduce engine out soot emissions. However, OME$_{3-5}$ is potentially damaging to engine components, and thus engine modifications are required when using neat OME$_{3-5}$.

In the present study, OME$_{3-5}$ was blended with hydrotreated vegetable oil (HVO), rapeseed methyl ester and the C$_8$-alcohol 2-ethylhexanol (an isomer of n-octanol) to ensure miscibility. Three blends were designed with an oxygen content of 6.4, 12.8 and 17.8% by mass. Performance and emissions were compared to the reference fuels fossil diesel and HVO in a single cylinder light duty and heavy duty compression ignition engine at different loads.

Evaluation of the combustion in both engines showed similar trends: The indicated thermal efficiency was slightly higher for the oxygenated fuel and the combustion duration shorter compared to diesel. Due to the lower heating value of the blends, the indicated specific fuel combustion increased with increasing share of OME$_{3-5}$ in the blend.

For both engines, engine out soot emissions were decreased strongly, whereas NO$_x$ emissions were slightly increased. Analysis of the particle size distribution showed a decrease in the particle number of agglomerated particles (>30 nm) for the blends. For the heavy duty engine, an increase in nucleation mode particles (<30 nm) was measured.

1. Introduction

Poly(oxymethylene)dimethyl ether (OME$_n$) has the general chemical structure CH_3-O-$(CH_2$-$O)_n$-CH_3, where n is the number of oxymethylene units. Recently, OME$_n$ has been suggested as an attractive fuel alternative for fossil diesel fuel in compression ignition (CI) engine research because it promises significant soot reduction for similar or slightly increased NO$_x$ levels. Thus, the typical soot-NO$_x$ trade off can be avoided. The main reason for this is the lack of carbon-to-carbon bonds and an oxygen mass fraction ranging from 42% by mass for OME$_1$ up to 50% by mass for OME$_n$ with $n > 1$ [1–4].

Several research studies have concluded that the combustion of OME$_1$ (also known as methylal or dimethoxymethane, DMM) in CI engines is soot free. However, OME$_1$ cannot be used as a drop-in fuel: modifications in engine hardware are required due to its high volatility, low flash point and low lubricity. Therefore, several researchers have suggested using blends of OME with $n > 1$, corresponding to mixtures of OME with n = 3–5 [5–8]. Thus, research efforts have concentrated mainly on OME$_{3-5}$ or higher. For example, Münz et al. tested pure OME$_{3-5}$ under real driving conditions (urban, rural and

motorway) with a SUV class vehicle equipped with a diesel particulate filter [9]. Using a portable emission measurement system, gaseous and particle emissions of OME$_{3-5}$ were compared to those of fossil diesel fuel. The main injection was changed to compensate for the smaller lower heating value (LHV) of OME$_{3-5}$. Particle number (PN) emissions were significantly lower than for diesel and below the current legislation

limit. Particle emissions were reduced by about 60% even under urban driving conditions [9]. Further, Iannuzzi et al. tested blends of OME_{2-6} with a share of 5% and 10% in diesel fuel in a single cylinder heavy duty engine with a single injection strategy [5]. Two load cases and variation of EGR and start of injection were investigated. With a share of 10% OME_{2-6}, a soot reduction of up to 34% could be achieved, while NO_x emissions and thermal efficiencies were not significantly affected. Due to the LHV of the blend, the break specific fuel consumption was increased [5]. Thus, OME_n has the potential to substitute fossil Diesel fuel. Disadvantages are the material compatibility [9,10] as well as the effect on the particle size distribution (PSD): An increase of small particles was found when using oxygenated fuels [11–14]. The correlation between PN emissions and respiratory disease is of particular concern, requiring limitations on PN emissions [15]. Thus, research on the PSD of oxygenated fuel emissions has increased.

Not only should the emissions of renewable fuels be significantly lower than for the fossil standard, but also the fuel production should be renewable in order to achieve low well-to-wheel emissions. Fuels for the present study were chosen based on the possibility of sustainable production. Fuel properties are presented in Table 1.

Neat fossil diesel fuel without added fatty acid methyl esters and HVO were used as a reference. The diesel fuel was sulfur free and had an aromatic content of < 8% by mass.

HVO is an aliphatic paraffinic hydrocarbon and is free of aromatic structures and sulfur. Properties of HVO resemble those of standard diesel, except HVO has a lower density and the CN is higher than for diesel. HVO can be produced from a wide range of feedstocks, including vegetable and animal wastes, palm oil, palm fatty acid distillate, soybean oil and tall oil (a by-product of the paper industry). The CN as well as cold start properties vary depending on the manufacturing process and can be adjusted [16,17].

OME can be produced from the platform chemical methanol. A detailed description of the production route can be found in [8,18]. The production costs of OME are highly dependent on the price of methanol but can be competitive to those of fossil diesel fuel [19,20].

2-Ethylhexanol (EH) is an isomer of *n*-octanol ($C_8H_{18}O$) containing 12.3% oxygen with a diesel-like density, a boiling point within the lower range of diesel and a low vapor pressure. EH was chosen because it can be produced from renewable resources and platform chemicals (ethanol) via thermochemical and biochemical conversion processes [21].

Rapeseed methyl ester (RME) consists of saturated and unsaturated fatty acids and can be produced by extraction of oil from rapeseeds, followed by a refining and transesterification reaction. RME is available in today's infrastructure, reduces well-to-wheel CO_2 emissions and promises a decrease in CO, HC and particulates whilst maintaining diesel-like properties, apart from the density and cold flow properties [22,23].

All components used had a flash temperature above 60 °C (333 K) under atmospheric conditions, which classifies all fuels in safety class IIIA [24].

The effect on combustion and emissions of blends containing different shares of OME_{3-5} were investigated in a light duty and heavy duty single cylinder CI engine. Reference fuels were fossil diesel and HVO. Blends with a maximum share of 27% OME_{3-5} by volume were used to avoid changes in hardware due to possible material incompatibility. The relationship between the oxygen content and the typical soot-NO_x trade off was examined. Further the PSD was investigated. Results are presented in Section 3 for the heavy duty engine and Section 4 for the light duty engine.

2. Experimental setup

2.1. Fuel blending strategy

The miscibility of OME depends strongly on the number of polyoxymethylene units in the polymer and the temperature. The OME used for this study mainly comprised OME_n $n = 3–5$. The composition by volume percent of the fuel was:

- 0.3% OME_2
- 46.8% OME_3
- 29.2% OME_4
- 16.6% OME_5
- 5.6% OME_6

At concentrations >30% by volume, OME_{3-5} did not mix with HVO at room temperature. Therefore, the long-chain alcohol 2-ethylhexanol and RME were added and the share of OME was kept below 27%.

The share of 7% RME by volume is standard in commercial diesel fuel, and the share of EH was kept for each blend at 10% by volume. The blends and associated densities, LHVs, oxygen content and cetane numbers are listed in Table 2. For OME_{3-5} and EH, 200 ppm of a lubricity agent (Trigonox B) was added. Basic compatibility experiments showed swelling of rubber parts and sealings. These observations agree with those of other research groups [7,9,10]. For example, Kass et al. investigated the compatibility of OME-diesel blends on elastomers [10]. Swelling of up to 33% in the volume of rubber components was found. They concluded that either rubber parts in the engine have to be adapted to resist OME_{3-5} blends or a low share of OME_{3-5} in the blend has to be used.

2.2. Engine settings

Experiments were performed on a heavy duty or light duty CI single cylinder research engine.

For the heavy duty engine tests, an AVL 501 single cylinder engine

Table 1
Properties of the blend components.

	Unit	Diesel	HVO	RME	2-Ethylhexanol	OME_{3-5}
Density (15 °C)	kg/m³	830	779.9	880	832	1066,5
Cetane number (CN)	–		52	75	52	23.2	54
Aromatic content	vol.%	5.2	–	–	–	–
Flash point	°C	74	94	120	75	63
Lower heating value (LHV)	MJ/kg	42.9	44.1	38.0	38.4	19.1
Oxygen content	m.%	–	–	10.8	12.3	43.1
$AFR_{stoichiometric}$		14.45	14.89	12.56	12.3	5.83
Boiling point	°C	180 – 350	180 – 320	317 – 346	184	117 – 241
Viscosity Kin. (40 °C)	mm²/s	3.0	2.6	4.4	5.2	1.18
Vapor pressure (25 °C)	kPa	<1.0	0.09	0.42	0.03	NA

Table 2
Composition of the fuel blends.

	unit	OME Blend 1	OME Blend 2	OME Blend 3
OME_{3-5}	vol.%	7	18	27
HVO	vol.%	76	65	56
RME	vol.%	7	7	7
2-Ethylhexanol	vol.%	10	10	10
Density	Kg/m³	808.9	840.4	866.2
Oxygen	m.%	6.4	12.8	17.8
$AFR_{stoichiometric}$	–	13.92	13.06	12.34
LHV	MJ/kg	40.75	37.40	34.84
CN	–	68.0	66.6	65.1

equipped with a cylinder head from a Volvo D13 was used. The light duty tests were performed with a Ricardo Hydra engine equipped with a Volvo NED4 cylinder head. Detailed engine specifications are shown in Table 3.

2.3. Engine equipment and analytic devices

2.3.1. Heavy duty

The fuel consumption was measured with an AVL 733S fuel balance. After passing through a conditioning unit, the fuel was injected with a common rail F2 injector from a Delphi fuel pump into the combustion chamber. A pressure sensor (Kistler 7061B) and piezo amplifier (Kistler 3066A01) were used to measure cylinder pressure data, which were sampled using Osiris data acquisition software. The engine was equipped with an AVL554 oil cooling unit and AVL553 water cooling unit.

Exhaust gas recirculation (EGR) was regulated with a valve in the exhaust pipe. The EGR value was calculated based on carbon dioxide emissions for the intake and exhaust.

Exhaust gas emissions were detected using the iGEM emission measurement system AVL AMA i60. NO_x emissions were measured with a chemiluminescence system. A flame ionization detector (FID) was used to evaluate unburned hydrocarbons. Carbon monoxide and carbon dioxide were measured with infrared detectors (IRD). A reproducibility of 0.5% of the full scale was obtained with each gas analyzer module..

The particle mass per cubic meter exhaust was measured with an AVL Micro Soot Sensor. This device uses a photoacoustic measuring principle to detect particle mass flow by exposing particles to modulated light. The expansion due to the temperature changes in the particles results in a sound wave that can be detected by means of microphones. The signal increases proportionally with the concentration of particles in the exhaust sample. The measurements had a resolution of 0.01 mg/m^3 with a measuring range of 0.001–50 mg/m^3.

To measure the PSD in the exhaust, a Cambustion DMS500 was used. Particles with diameters between 5 nm and 1000 nm were able to be classified. The gas sample passed a corona charger before entering a classifier column. The particles adopted positions in the column according to their charge and aerodynamic drag. An amplifier converted the resulting currents into number and size data of the particles. The dilution factor for the measurements was kept constant at 6:1, because particle size measurements strongly depend on the dilution conditions [25]. A second dilution factor was assigned to maintain a good signal to noise ratio. For all cases, the 2nd dilution factor was set to 12. Samples for both the Micro Soot Sensor and DMS500 were taken at the exhaust tailpipe. Table 4 summarizes the used measurement devices and the corresponding accuracies.

2.3.2. Light duty

A Denso injector produced up to four injections per cycle. An AVL 730 fuel balance was used to measure the fuel mass flow. The in-cylinder pressure was measured by an AVL GUI2S-10 pressure transducer, amplified by a Kistler 5011 piezo amplifier and detected with an AVL IndiCom system. A resolution of 0.2 CAD was used. NO_x emissions were measured using a Rosemount CLD 951A with an accuracy of $< 5\%$ of the full scale. A Rosemount Binos 1001/1004 instrument was used to measure the concentration of $CO_{2, intake}$ and $CO_{2, exhaust}$ with an accuracy

Table 3
Engine specifications.

	Heavy duty	Light duty
Engine type	AVL 501	Ricardo Hydra
Cylinder head	Volvo D13	Volvo NED4
Displacement volume, dm^3	2.13	0.49
Bore, mm	131	82
Stroke, mm	158	93
Compression ratio	17:1	15.8:1
Fuel injection system	Common rail	Common rail

Table 4
Measurement equipment for the HD setup.

	Equipment	Accuracy
$CO_{2,intake}$ $CO_{2,exhaust}$	IRD AMA i60	<0.5% of the full scale
NO_x	CLD AMA i60	<5% of the full scale
PM	AVL Micro Soot Sensor	0.01 mg/m^3
PN	Cambustion DMS500	<5% in general
Fuel consumption	AVL 733S	0.12%

Table 5
Measurement equipment for the LD setup.

	Equipment	Accuracy
$CO_{2,intake}$ $CO_{2,exhaust}$	Rosemount Binos 1001/1004	<2% of the full scale
NO_x	Rosemount CLD 951A	<5% of the full scale
PM	AVL Micro Soot Sensor	0.01 mg/m^3
PN	Cambustion DMS500	<5% in general
Fuel consumption	AVL 730	<1%

of $< 2\%$ of the full scale. The EGR value was calculated based on the carbon dioxide emissions for the intake and exhaust. Particle mass emissions were measured with an AVL Micro Soot Sensor and PN emissions with the Cambustion DMS500, as described earlier. The primary dilution factor for the measurements was kept constant at 6:1 and the second dilution factor was set to 48 for all cases.

Table 5 summarizes the used measurement devices and the corresponding accuracies.

2.4. Operation conditions

2.4.1. Heavy duty

To compare the performance of the different fuel mixtures, fossil diesel fuel (without fatty acid methyl esters, FAME) was used as a reference fuel. Four load points from the European Stationary Cycle (ESC) were used: A25, B50, B75 and C75. The chosen reference point B50 was run at the beginning and between each test cycle to evaluate changes in engine performance over time. Table 6 lists the engine parameters adapted from the factory settings for a production engine. The injection duration is shown for diesel fuel. Due to the lower LHV of the fuel blends, the injection duration was adjusted to maintain constant torque. The EGR system had an accuracy of $\pm$ 0.1% unit.

To change the fuel, the fuel balance system including fuel filters was emptied and flushed with the new fuel. Before starting each measurement, the engine was run for at least one hour to minimize any contamination from previous fuel tests.

2.4.2. Light duty

Three representative load cases were chosen for the light duty engine tests (Table 7). Fuel was injected with a multi-injection strategy: double-pre/main/post – injection. To compensate for the different LHV of the fuels (Table 2), the double-pre injection and main injection durations were adjusted. All load cases were repeated three times. Data for emissions are presented as averages over two minutes.

Table 6
Operating conditions for heavy duty engine tests.

	Unit	A25	B50	B75	C75
Speed	r/min	1200	1500	1500	1800
IMEPnet	MPa	0.64	1.11	1.61	1.40
Injection timing	BTDC	4.52	7.8	9.4	4.5
Injection duration	μs	668	1060	1466	1346
Injection pressure	MPa	180	180	180	180
EGR	%	16.5	12.9	12.5	17.7

Table 7

Operating conditions for light duty engine tests.

	Unit	1	2	3
Speed	r/min	1280	1810	2000
IMEP	MPa	0.88	0.72	1.12
Pre injection 1	BTDC	7.2	17.6	17.0
Pre injection 2	BTDC	2.8	10.6	10.0
Main injection	BTDC	−3.2	3.6	2.4
Post injection	BTDC	−12.6	−9.0	−13.0
Injection pressure	MPa	7.93	6.69	9.11
EGR	%	19.4	27.3	22.5
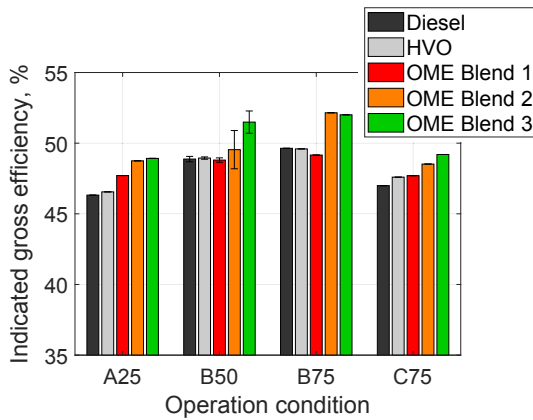
3. Results for heavy duty engine tests

3.1. Engine performance

To analyze and compare the results for the three oxygenated fuels blends to diesel and HVO, bar diagrams were used. In these diagrams, the first two bars for each load case represent diesel (black) and HVO (gray), whereas the three remaining bars show the OME blends in order of increasing oxygen content.

Compared to diesel, the indicated specific fuel consumption (ISFC) for HVO decreased in average by 2.8%. Owing to the lower LHV of the blends, the injection duration was increased. Thus, ISFC increased in
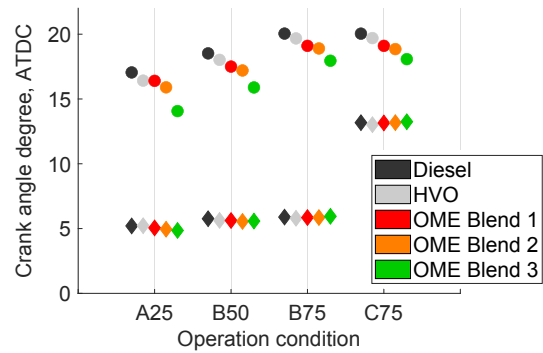

Fig. 1. Heavy duty engine: indicated thermal efficiency.

Fig. 3. Heavy duty engine: MFB50 (◆) and combustion duration (●) timing in CAD ATDC.
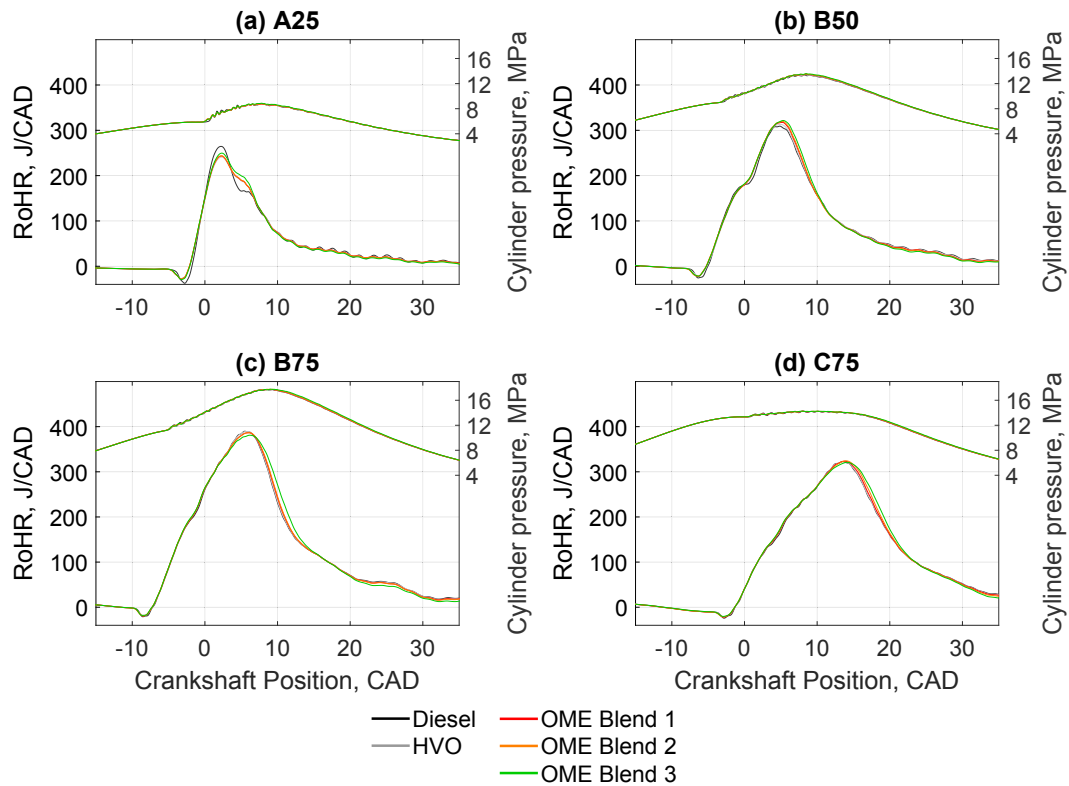

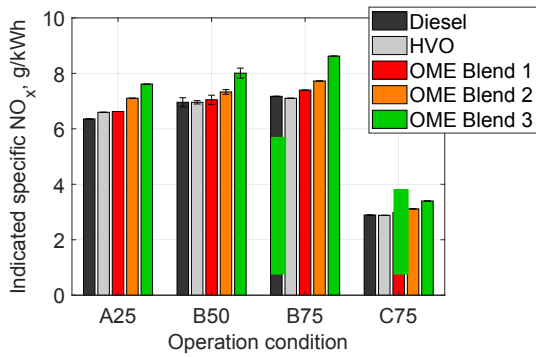**Fig. 2.** Heavy duty engine: Cylinder pressure and rate of heat release.

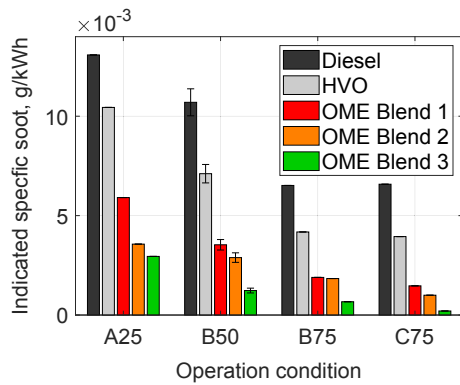**Fig. 4.** Heavy duty engine: Indicated specific NO$_x$ emissions.

Fig. 5. Heavy duty engine: Indicated specific soot emissions.

average by 6.4%, 11.3% and 20.5% for OME Blend 1–3, respectively.

The indicated gross efficiency is shown in Fig. 1 for all four load cases. Diesel and HVO had similar indicated efficiencies.

At the low load case (A25), the efficiency of OME Blend 1 was higher than that of diesel and HVO but similar for middle and high load cases when considering the standard deviation. OME Blend 2 and 3 showed

increased efficiencies with increasing share of OME for all load cases.

The cylinder pressure and rate of heat release are shown in Fig. 2.

The combustion analysis revealed a similar timing for MFB50 (crank angle where 50% of the fuel has burned) for all fuels, whereas the combustion duration differed, as shown in Fig. 3. HVO burned slightly faster than diesel, and the combustion duration of the blends decreased with increasing share of oxygen (increasing proportion of OME) in the blend. The shortened time of MFB90-MFB50 may be one reason for the increased efficiency of the blends and has been observed previously in similar OME engine tests by Dworschak et al. [14]. However, heavy duty engine tests by Dworschak et al. were performed with OME$_{2-6}$ and without EGR.

Exhaust gas temperatures and heat losses decreased with increasing proportion of OME in the blend. Heat losses for OME Blend 1 were comparable with HVO and OME, and thus the efficiencies were similar.

Comparing the high load cases B75 and C75, MFB50 occurred later for C75 than B75 due to the retarded start of injection.

3.2. Exhaust gas emissions

CI engines are known to be highly efficient. However, when using fossil diesel fuel, soot and NO$_x$ emissions are generally high. Current research on renewable fuels aims to decrease emissions to improve air quality.

Fig. 4 shows NO$_x$ emissions for all the blends compared to diesel. As expected, NO$_x$ emissions increased with increasing proportion of oxygen in the fuel blend. Diesel and HVO emitted comparable NO$_x$ emissions. For OME Blend 3, NO$_x$ emissions were increased by 18% compared to diesel fuel. Load C75 had lower NO$_x$ emissions due to the late MFB50. The retarded combustion leads to lower in-cylinder temperatures.

Results for soot emissions are shown in Fig. 5. The specific soot mass of HVO was lower than for diesel due to the lack of aromatic structures in HVO.

As expected, soot emissions decreased with increasing share of OME. The reduction was especially significant for the high load case C75: from 78% for OME Blend 1 to 97% for OME Blend 3.

In earlier experiments with long-chain alcohol - HVO blends and comparable engine settings, soot mass was found to be decreased [26]. A
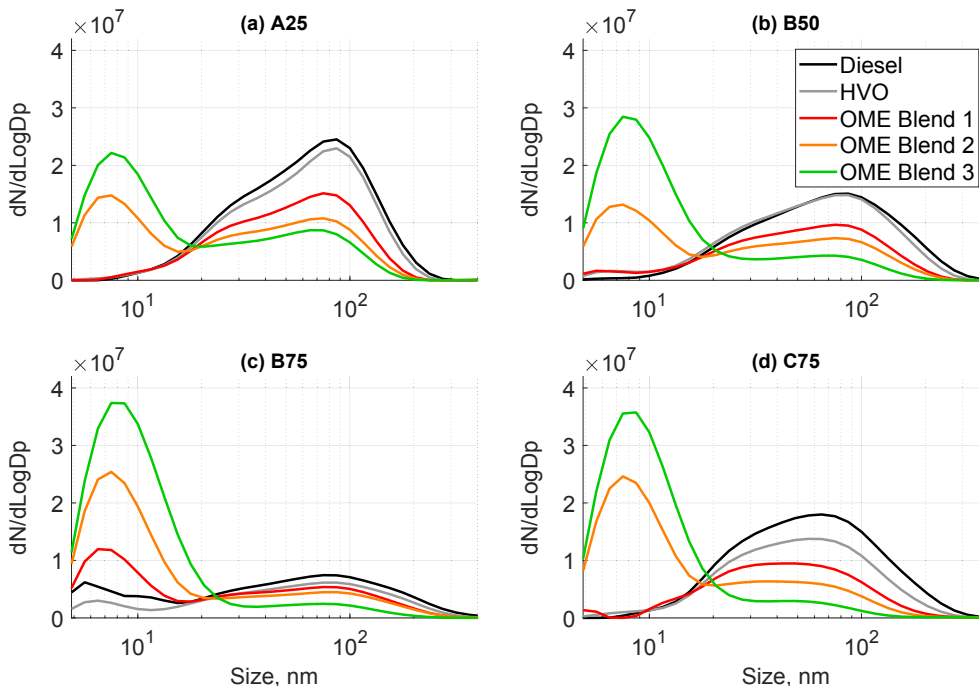

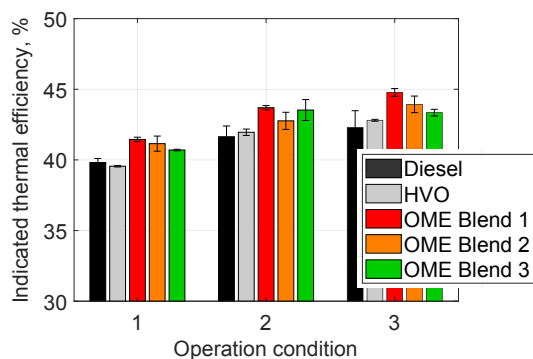**Fig. 6.** Heavy duty engine: Particle size distribution.

Fig. 7. Light duty engine: Indicated thermal efficiency.

blend with a volumetric share of 43% 2-ethylhexanol, 50% HVO and 7% RME has an oxygen content of 6.0% by mass. Compared to OME Blend 1, which has an oxygen content of 6.4% by mass (Table 2), the reduction in soot was higher for the OME blend. Both the HVO blend and OME Blend 1 have a similar density, LHV and do not contain aromatic structures (e. g., polycyclic aromatic hydrocarbons, PAHs), which are known soot precursors. Therefore, a probable explanation for the higher soot reduction with OME Blend 1 is the lack of carbon–carbon bonds in OME. Moreover, OME blends have a higher CN, thus the ignition delay differed.

3.3. Particulate emissions

The use of renewable fuel alternatives alters the nature of emitted particles. The PSD of diesel exhaust is often bimodal, and typically particles are divided into modes according to their diameter. Nucleation mode particles are formed by the nucleation of volatile particles and have a size range of 0 to 30 nm. Particles above this range are referred to as accumulation mode, where particles consist of carbon-based agglomerates. Particles in the nucleation mode cover up to 10% of the particle mass. The rest are represented by particles in the accumulation mode [27–31].

The PSDs for the different fuels and load cases are shown in Fig. 6. Compared to diesel, HVO showed a slightly lower PN. For the B50 load case, diesel particles were higher in number at diameters > 100 nm. With increasing share of OME in the blends, the number of particles in the accumulation mode (>30 nm) decreased, whereas the number of small particles in the nucleation mode (<30 nm) increased. OME Blend 1 did not show an increase in nucleation mode particles compared to diesel and HVO for load cases A25 and B50 and showed only a small increase for the higher load cases B75 and C75. However, there was a decrease in agglomeration particles.

The nature of the small particles is unknown. Previous research has suggested that the peak in small particle sizes is due to volatiles from lubrication oil [32]. One reason for the increase in nucleation mode particles may be the increased injection duration (to compensate for the lower LHV) or lower exhaust gas temperatures, which favor nucleation mode particles [33]. Another reason may be a change in particle morphology with change in fuel blend composition. Research on soot structure and nanoparticle morphology has shown that oxygenated fuels produce soot particles with a more amorphous structure, which enhances soot oxidation. Thus, the surface growth of particles is reduced, resulting in smaller geometric mean particle diameters [34,35]. Dworschak et al. found the PSD of neat OME_{2-6} load dependent: At low and high engine load of a heavy duty engine without EGR, a formation of nucleation mode was observed. Because, there were no nucleation mode particles observed at medium load, it was concluded that the influence on the PSD lies not only on the fuel properties but correlates with engine operation conditions. Those can be for example an extended injection duration at high loads or low exhaust temperatures at low loads [14].

4. Results for light duty engine tests

4.1. Engine performance

Compared to diesel, the indicated specific fuel consumption (ISFC) for HVO was decreased in average by 2.5%. Owing to the lower LHV of the blends, the injection duration was increased. Thus, the ISFC was increased in average by 2.3%, 16.7% and 24.8% for the OME Blends 1–3, respectively.

Fig. 7 shows the indicated thermal efficiency. Diesel and HVO had similar efficiencies, whereas the blends had a slightly higher efficiency. However, when considering standard deviation, no distinct trend was detected among the blends.

The cylinder pressure and rate of heat release are plotted in Fig. 8. With increasing content of OME_{3-5}, the cylinder pressure increased compared to that of diesel. Moreover, the ignition delay was shorter in the pre-injection for the blends due to their higher CN (Table 2). However, the main combustion started at a similar crank angle. Fig. 9 shows the timing where 50% of the mass fraction was burned (MFB50) and the combustion duration (MFB90 – MFB10). For load 1 and 2, MFB50 was slightly earlier for the blends, whereas the combustion duration decreased with increasing share of OME. Thus, heat losses in the exhaust were decreased, which contributed to the higher efficiency (Fig. 7). At the higher load case (load 3), MFB50 was similar for all the fuels but the combustion duration was slightly shorter for the blends.
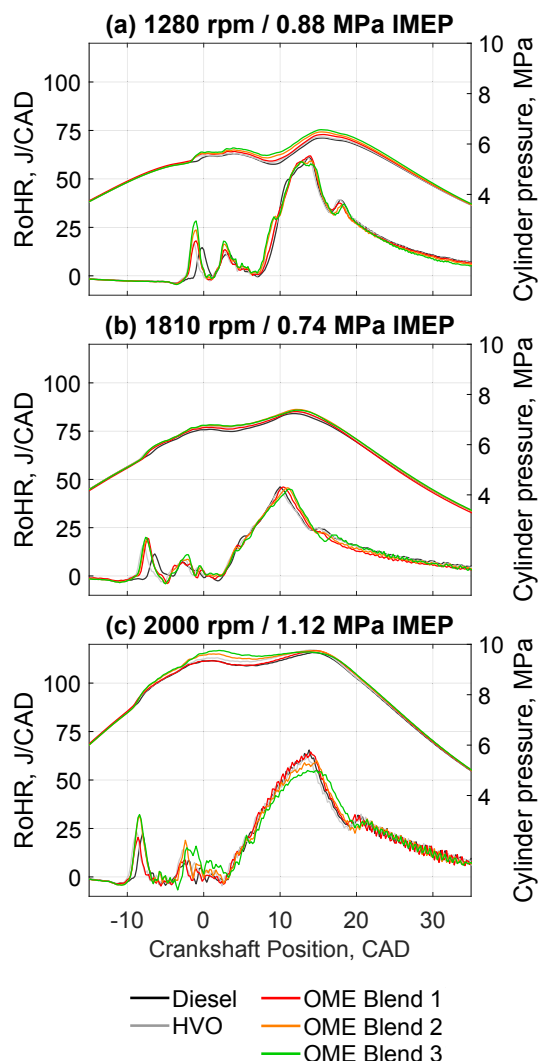

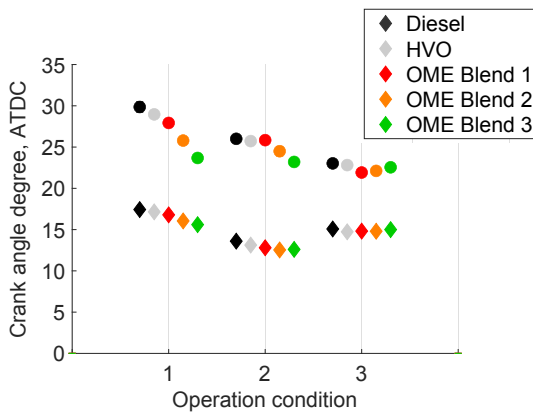**Fig. 8.** Light duty engine: Cylinder pressure and rate of heat release.

Fig. 9. Light duty engine: MFB50 (◆) and combustion duration (●) timing in CAD ATDC.
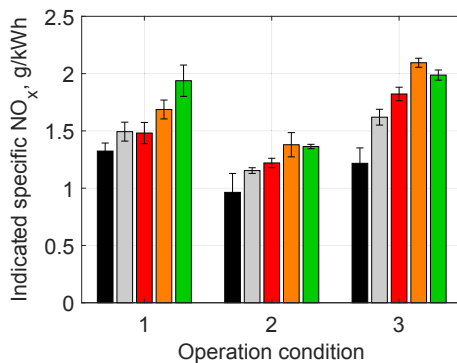

Fig. 10. Light duty engine: Indicated specific NO$_x$.

4.2. Exhaust gas emissions

Results for the indicated specific NO$_x$ and indicated specific soot mass emissions are presented in Fig. 10 and Fig. 11, respectively. While soot mass emissions of HVO were about half those of diesel, NO$_x$ emissions were increased slightly. For OME Blend 1, NO$_x$ emissions were similar to those of HVO for the lower load cases (load 1 and 2) when considering the standard deviation. Soot emissions for OME Blend 1 were about one third those of diesel for the medium load case (load 1) and were comparable to those of HVO for higher load cases.

The soot reduction potential of the blends decreased with increasing load, in agreement with results reported in the literature [14]. For OME Blend 2 and 3, NO$_x$ emissions increased, whereas soot emissions decreased strongly with increasing OME content.
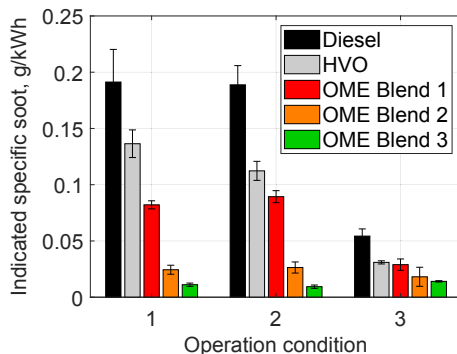

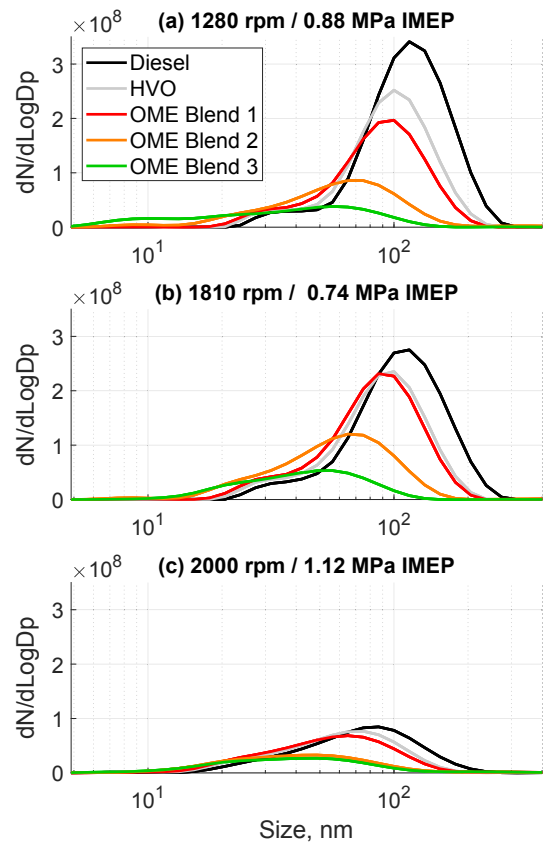**Fig. 11.** Light duty engine: Indicated specific soot.

Fig. 12. Light duty engine: Particle size distribution.

4.3. Particulate emissions

Fig. 12 shows the PSDs for the different fuels and load cases. Exhaust particle emissions from renewable fuels vary not just in quantity but also their particle number and size. Correspondent to the soot mass emissions, PN decreased with increasing share of OME in the blends. Moreover, the geometric mean particle diameter was reduced. The PSD for OME Blend 1 differed only slightly from that of HVO. The lowest PN emissions were at the highest load. There was a very low number of particles in the nucleation mode. This was probably due to the multi-injection strategy [36]. The results from the particle size measurements agree with those from the soot mass measurements.

5. Summary and conclusion

The effect of using three blends containing OME$_{3-5}$, HVO, RME and the C$_8$-alcohol 2-ethylhexanol was investigated in a heavy duty and light duty CI engine at different loads. The OME blends were designed to have an oxygen content of 6.4, 12.8 and 17.8% by mass. Fossil diesel fuel and HVO were used as reference fuels. Compared to diesel and HVO, the LHVs of the blends were lower. Thus, the injection duration was adjusted to ensure a constant engine load. Consequently, the indicated specific fuel consumption increased with increasing OME content in the blend.

The following results on performance and emissions were observed:

- For the heavy duty engine, the ISFC increased by 6.4%, 11.3% and 20.5% for OME Blends 1–3, respectively, in relation to diesel. For the light duty engine, the ISFC increased in average by 2.3%, 16.7% and 24.8% for OME Blends 1–3, respectively.
- The trends in efficiency as well as soot and NO$_x$ emissions were similar for both engines: The indicated efficiencies were higher for

OME Blends 2 and 3 than for diesel and HVO, whereas the efficiency of OME Blend 1 was similar to those of the reference fuels.

- Faster combustion (shorter combustion duration, MFB90-MFB10) led to lower exhaust gas temperatures, and thus lower heat losses in the exhaust. Soot emissions were strongly reduced for the blends, whereas NO_x emissions were increased slightly.
- When using the oxygenated blends, a large number of particles in the heavy duty exhaust were in the nucleation mode, which might cause difficulties in satisfying future legislation on PN (>10 nm). The nucleation mode PN increased with increasing share of OME.
- For the light duty engine exhaust, the PNs of the blends were lower than that of diesel. The number of particles in the nucleation mode was very low due to the multiple injection strategy.

Overall, the results showed that blends containing OME_{3-5}, HVO, RME and a long-chain alcohol (octanol) can be used as a drop-in fuel in light and heavy duty CI engines.

The tested OME_{3-5} blends allowed the engine to run without hardware modifications. However, further research is needed to investigate material compatibility when using fuel blends with different proportions of OME.

CRediT authorship contribution statement

Josefine Preuß: Conceptualization, Formal analysis, Investigation, Methodology, Visualization, Writing - original draft. **Karin Munch:** Conceptualization, Methodology, Resources, Writing - review & editing. **Ingemar Denbratt:** Conceptualization, Funding acquisition, Project administration, Supervision, Writing - review & editing.

Declaration of Competing Interest

The authors declare that they have no known competing financial interests or personal relationships that could have appeared to influence the work reported in this paper.

References

[1] Iannuzzi SE, Barro C, Boulouchos K, Burger J. Combustion behavior and soot formation/oxidation of oxygenated fuels in a cylindrical constant volume chamber. Fuel 2016;167:49–59. https://doi.org/10.1016/j.fuel.2015.11.060.

[2] Omari A, Heuser B, Pischinger S, Rüdinger C. Potential of long-chain oxymethylene ether and oxymethylene ether-diesel blends for ultra-low emission engines. Appl Energy 2019;239:1242–9. https://doi.org/10.1016/j.apenergy.2019.02.035.

[3] Dworschak P, Berger V, Härtl M, Wachtmeister G. Neat Oxymethylene Ethers: Combustion Performance and Emissions of OME2, OME3, OME4 and OME5 in a Single-Cylinder Diesel Engine. SAE Tech Pap 2020;2020-April:1–13. 10.4271/2020-01-0805.

[4] Barro C, Parravicini M, Boulouchos K. Neat polyoxymethylene dimethyl ether in a diesel engine; part 1: Detailed combustion analysis. Fuel 2019;256:115892. https://doi.org/10.1016/j.fuel.2019.115892.

[5] Iannuzzi SE, Barro C, Boulouchos K, Burger J. POMDME-diesel blends: Evaluation of performance and exhaust emissions in a single cylinder heavy-duty diesel engine. Fuel 2017;203:57–67. https://doi.org/10.1016/j.fuel.2017.04.089.

[6] Härtl M, Seidenspinner P, Jacob E, Wachtmeister G. Oxygenate screening on a heavy-duty diesel engine and emission characteristics of highly oxygenated oxymethylene ether fuel OME1. Fuel 2015;153:328–35. https://doi.org/10.1016/j.fuel.2015.03.012.

[7] Omari A, Heuser B, Pischinger S. Potential of oxymethylenether-diesel blends for ultra-low emission engines. Fuel 2017;209:232–7. https://doi.org/10.1016/j.fuel.2017.07.107.

[8] Burger J, Siegert M, Ströfer E, Hasse H. Poly (oxymethylene) dimethyl ethers as components of tailored diesel fuel : Properties, synthesis and purification concepts. Fuel 2010;89:3315–9. https://doi.org/10.1016/j.fuel.2010.05.014.

[9] Münz M, Mokros A, Töpfer D, Beidl C. OME – Assessment of Particle Emissions in Real Driving Conditions. MTZ Worldw 2018;79(3):16–21.

[10] Kass M, Wissink M, Janke C, Connatser R, Curran S. Compatibility of Elastomers with Polyoxymethylene Dimethyl Ethers and Blends with Diesel. SAE Int J Adv Curr Pr Mobil 2020–01-0620 2020;2:1963–73. https://doi.org/10.4271/2020-01-0620.

[11] Barro C, Parravicini M, Boulouchos K, Liati A. Neat polyoxymethylene dimethyl ether in a diesel engine; part 2: Exhaust emission analysis. Fuel 2018;234:1414–21. https://doi.org/10.1016/j.fuel.2018.07.108.

[12] Pepiot-Desjardins P, Pitsch H, Malhotra R, Kirby S, Boehman A. Structural group analysis for soot reduction tendency of oxygenated fuels. Combust Flame 2008;154 (1-2):191–205. https://doi.org/10.1016/j.combustflame.2008.03.017.

[13] Desantes JM, Bermúdez V, García JM, Fuentes E. Effects of current engine strategies on the exhaust aerosol particle size distribution from a Heavy-Duty Diesel Engine. J Aerosol Sci 2005;36(10):1251–76. https://doi.org/10.1016/j.jaerosci.2005.01.002.

[14] Dworschak P, Berger V, Härtl M, Wachtmeister G. Measurements of Neat and Water-Emulsified Oxymethylene Ethers in a Heavy-Duty Diesel Engine. SAE Int J Fuels Lubr 04–13-02-0012 2020;13:187–203. https://doi.org/10.4271/04-13-02-0012.

[15] Giechaskiel B, Vanhanen J, Väkevä M, Martini G. Investigation of vehicle exhaust sub-23 nm particle emissions. Aerosol Sci Technol 2017;51(5):626–41. https://doi.org/10.1080/02786826.2017.1286291.

[16] Swedish Energy Agency. Energy in Sweden-Fact and Figures 2015 2015.

[17] Neste Oil. Hydrotreated vegetable oil (HVO)-premium renewable biofuel for diesel engines 2014.

[18] Burger J, Ströfer E, Hasse H. Chemical equilibrium and reaction kinetics of the heterogeneously catalyzed formation of poly(oxymethylene) dimethyl ethers from methylal and trioxane. Ind Eng Chem Res 2012;51(39):12751–61. https://doi.org/10.1021/ie301490q.

[19] Schmitz N, Burger J, Ströfer E, Hasse H. From methanol to the oxygenated diesel fuel poly(oxymethylene) dimethyl ether: An assessment of the production costs. Fuel 2016;185:67–72. https://doi.org/10.1016/j.fuel.2016.07.085.

[20] Bokinge P, Heyne S, Harvey S. Renewable OME from biomass and electricity—Evaluating carbon footprint and energy performance. Energy Sci Eng 2020;8(7):2587–98. https://doi.org/10.1002/ese3.687.

[21] Munch K, Zhang T. A Comparison of Drop-In Diesel Fuel Blends Containing Heavy Alcohols Considering Both Engine Properties and Global Warming Potentials. SAE Tech Pap 2016-01-2254 2016. 10.4271/2016-01-2254.Copyright.

[22] Perstorp BioProducts AB. Safety data sheet RME - Perstorp BXN, according to 1907/2006/EC, Article 31. 2016.

[23] Johansson M. Fischer-Tropsch and FAME Fuels as Alternatives for Diesel Engines; an Experimental Study 2012.

[24] National Fire Protection Association. NFPA 30: Flammable and Combustible Liquids Code. 2018.

[25] Rönkkö T, Virtanen A, Vaaraslahti K, Keskinen J, Pirjola L, Lappi M. Effect of dilution conditions and driving parameters on nucleation mode particles in diesel exhaust: Laboratory and on-road study. Atmos Environ 2006;40(16):2893–901. https://doi.org/10.1016/j.atmosenv.2006.01.002.

[26] Preuß J, Munch K, Denbratt I. Performance and emissions of long-chain alcohols as drop-in fuels for heavy duty compression ignition engines. Fuel 2018;216:890–7. https://doi.org/10.1016/j.fuel.2017.11.122.

[27] Giechaskiel B, Martini G. Engine Exhaust Solid Sub-23 nm Particles: II. Feasibility Study for Particle Number Measurement Systems. SAE Int J Fuels Lubr 2014-01-2832 2014;7:2014-01–2832. 10.4271/2014-01-2832.

[28] Kittelson D, Watts W, Johnson J. Diesel Aerosol Sampling Methodology - CRC E-43: Executive Summary. Tech Summ Conclusion. University Minnesota; 2002.

[29] Rönkkö T, Virtanen A, Kannosto J, Keskinen J, Lappi M, Pirjola L. Nucleation mode particles with a nonvolatile core in the exhaust of a heavy duty diesel vehicle. Environ Sci Technol 2007;41(18):6384–9. https://doi.org/10.1021/es0705339.

[30] May J, Bosteels D, Such C, Nicol A, Andersson J. Heavy-duty Engine Particulate Emissions: Application of PMP Methodology to measure Particle Number and Particulate Mass. SAE Tech Pap 2008-01-1176 2008. 10.4271/2008-01-1176.

[31] Kittelson DB. Engines and nanoparticles: A review. J Aerosol Sci 1998;29(5-6): 575–88. https://doi.org/10.1016/S0021-8502(97)10037-4.

[32] Shamun S, Novakovic M, Malmborg VB, Preger C, Shen M, Messing ME, et al. Detailed characterization of particulate matter in alcohol exhaust emissions. COMODIA 2017 - 9th Int Conf Model Diagnostics Advanved Engine Syst 2017. 10.1299/jmsesdm.2017.9.b304.

[33] Kittelson D, Kraft M. Particle Formation and Models in Internal Combustion Engines. Encycl. Automot. Eng. 2014. https://doi.org/10.1002/9781118354179.auto161.

[34] Boehman AL, Song J, Alam M. Impact of biodiesel blending on diesel soot and the regeneration of particulate filters. Energy Fuels 2005;19(5):1857–64. https://doi.org/10.1021/ef0500585.

[35] Xu Z, Li X, Guan C, Huang Z. Characteristics of exhaust diesel particles from different oxygenated fuels. Energy Fuels 2013;27(12):7579–86. https://doi.org/10.1021/ef401946t.

[36] Desantes JM, Bermúdez V, García A, Linares WG. A comprehensive study of particle size distributions with the use of postinjection strategies in DI diesel engines. Aerosol Sci Technol 2011;45(10):1161–75. https://doi.org/10.1080/02786826.2011.582898.